Journal of Applied Fluid Mechanics, Vol. 9, No. 3, pp. 1447-1455, 2016.
Available online at www.jafmonline.net, ISSN 1735-3572, EISSN 1735-3645.
DOI: 10.18869/acadpub.jafm.68.228.24135

Soret and Dufour Effects on MHD Mixed Convection Heat and Mass Transfer of a Stagnation Point Flow towards a Vertical Plate in a Porous Medium with Chemical Reaction, Radiation and Heat Generation

S. Karthikeyan[1], M. Bhuvaneswari[2], S. Sivasankaran[2†] and S. Rajan[1]

[1] *Department of Mathematics, Erode Arts and Science College, Erode 638009, Tamilnadu, India*
[2]*Institute of Mathematical Sciences, University of Malaya, Kuala Lumpur 50603, Malaysia*

†*Corresponding Author Email: sd.siva@yahoo.com (corresponding author)*

(Received October 7, 2014; accepted April 15, 2015)

ABSTRACT

The objective of this paper is to analyze the effects of heat and mass transfer in the presence of thermal radiation, internal heat generation and Dufour effect on an unsteady magneto-hydrodynamic mixed convection stagnation point flow towards a vertical plate embedded in a porous medium. The non-linear partial differential equations governing the flow are transformed into a set of ordinary differential equations using suitable similarity variables and then solved numerically using shooting method together with Runge-Kutta algorithm. The effects of the various parameters on the velocity, temperature and concentration profiles are depicted graphically and values of skin- friction coefficient, Nusselt number and Sherwood number for various values of physical parameters are tabulated and discussed. It is observed that the temperature increases for increasing values of the internal heat generation, thermal radiation and the Dufour number and hence thermal boundary layer thickness increases.

Keywords: Stagnation point flow; Mixed convection; Porous medium; Heat generation; Thermal radiation.

NOMENCLATURE

B_0	strength of magnetic field
C	concentration of the fluid
c_p	specific heat
c_s	concentration susceptibility
Df	Dufour number
D_m	diffusion coefficient
g	acceleration due to gravity
Gr	Thermal Grashof number
Gc	Solutal Grashof number
k	thermal conductivity
K	permeability parameter
K'	mean absorption coefficient
K_1	chemical reaction
$\tilde{K}$	permeability of the porous medium
K_T	thermal diffusion ratio
M	magnetic field parameter
Nu	Nusselt number
Pr	Prandtl number
S	heat generation/absorption parameter
Ri_C	Solutal Richardson number
Sc	Schmidt number
Sh	Sherwood number
Sr	Soret number
T	temperature of the fluid
(u, v)	velocity components
(x, y)	cartesian coordinates
α	thermal diffusivity
β	thermal expansion coefficient
β^*	concentration expansion coefficient
η	dimensionless variable
θ	dimensionless temperature
μ	viscosity
ν	kinematic viscosity
ρ	density
σ	electrical conductivity
σ^*	Stefan-Boltzmann constant
σ_e	fluid electrical conductivity

Q	heat generation/absorption coefficient
q_r	radiative heat flux
R	radiation parameter
Re_x	Reynolds number
Ri_T	Thermal Richardson number
φ	heat source parameter
ψ	stream function

Subscripts

w	at wall
∞	at free stream

1. INTRODUCTION

Heat and mass transfer by natural convection in a fluid-saturated porous medium has always been an active area of research due to the plenty of applications such as oil recovery, geothermal reservoirs, drying of porous solids and cooling of nuclear reactors. The flow in the neighborhood of a stagnation line has attracted many researchers during the last century. Stagnation-point flows may be produced by a solid wall, while in other cases a free stagnation point or line exists in the fluid domain. Hiemenz (1911) made the first contribution in this direction by examining the two-dimensional flow of a fluid near a stagnation point and obtained an exact similarity solution of the governing equations. Thermal effects in such a flow were introduced by Eckert (1942). The analysis by Devi *et al.* (1991) presented the unsteady mixed convection in stagnation point flows for arbitrary distribution of surface temperature and concentration or surface heat and mass flux conditions. They found that dual solutions exist for a certain range of the buoyancy parameter when the flow is opposing.

The effect of radiation on MHD flow and heat transfer problems has become industrially more important. Many engineering processes occur at high temperatures and hence the knowledge of radiation heat transfer is essential for designing appropriate equipment. In designing some of the complex equipments such as Nuclear power plants, gas turbines and various propulsion devices for aircrafts, the knowledge of radiation heat transfer becomes essential. In view of these, many authors have made contributions to the study of fluid flow with thermal radiation. The problem of radiative natural convection heat transfer flow past an inclined surface embedded in a porous medium is investigated by Lee *et al.* (2008). They observed that velocity increases and temperature decreases by increasing porosity parameter. Later, this work has been extended by Bhuvaneswari *et al.* (2012). They have analyzed this problem with the inclusion of internal heat generation and found that both the velocity and temperature increase significantly when the value of the heat generation parameter increases. Karthikeyan *et al.* (2013) have studied the influence of thermal radiation on magneto-convection flow of an electrically conducting fluid past a semi-infinite vertical porous plate embedded in a porous medium with time dependent suction. Radiation effects on boundary layer flow and heat transfer of a fluid with variable viscosity along a symmetric wedge is investigated by Mukhopadhyay (2009). Babu *et al.* (2014) have analyzed the steady MHD boundary layer flow due to an exponentially stretching sheet with radiation in the presence of mass transfer and heat source or sink.

Convective heat and mass transfer with chemical reaction plays an important role in meteorological phenomena, burning of haystacks, spray drying of milk, fluidized bed catalysis and cooling towers. Bhuvaneswari *et al.* (2009) examined the convective flow, heat and mass transfer of an incompressible viscous fluid past a semi-infinite inclined surface with first-order homogeneous chemical reaction by Lie group analysis. Soret and Dufour effects on similarity solution of hydro magnetic heat and mass transfer over a vertical plate with a convective surface boundary condition and chemical reaction are studied by Gangadhar (2013). Lie group analysis of natural convection over an inclined semi-infinite plate with variable thermal conductivity is investigated by Bhuvaneswari and Sivasankaran (2014). They observed that the velocity and temperature for all angles increase when the thermal conductivity parameter increases. An analysis of visco-elastic free convective MHD flow over a vertical porous plate through porous media in presence of radiation and chemical reaction is presented by Choudhury and Kumar Das (2014). An investigation of the effects of Hall current and rotation on unsteady hydro-magnetic natural convection flow with heat and mass transfer of an electrically conducting, viscous, incompressible and time dependent heat absorbing fluid past an impulsively moving vertical plate in a porous medium taking thermal and mass diffusions into account is carried out by Seth *et al.* (2015). Various aspects of stagnation-point flow and heat transfer have been studied by many researchers and thus a considerable literature have been generated on this domain. The problem of the flow near a stagnation point of a heated surface embedded in a fluid saturated porous medium has been subject of several numerical and analytical studies. Simultaneous heat and mass transfer by natural convection in a two dimensional stagnation-point flow of a fluid saturated porous medium, using the Darcy–Boussinesq model, including suction/blowing, Soret and Dufour effects are studied by Postelnicu (2010). There has been many works related to mixed convection flow near the stagnation point on a vertical surface/plate in a porous medium. The problem of unsteady mixed convection boundary layer flow near the region of a stagnation point on a heated vertical surface embedded in a fluid-saturated porous medium is considered by Nazar *et al.* (2004).

The stagnation-point flow due to a stretching sheet has received much attention because of its significance in industry, such as, extrusion of

polymers, glass fiber, the cooling of metallic plate and the aerodynamics. Further, the inclusion of magnetic field in the study of stagnation point flow has many practical applications, for example, the cooling of turbine blades, where the leading edge is a stagnation point, or cooling the nose cone of the rocket during re-entry. Hayat *et al*. (2010) analyzed the problem of steady MHD two-dimensional mixed convection boundary layer flow of a viscous and incompressible fluid near the stagnation-point on a vertical stretching surface embedded in a fluid-saturated porous medium and thermal radiation. A study on the effects of heat generation/absorption and chemical reaction on unsteady MHD flow heat and mass transfer near a stagnation point of a three dimensional porous body in the presence of a uniform magnetic field is presented by Chamkha *et al.* (2011). Sharma and Singh (2009) have investigated the effects of variable thermal conductivity, heat source/sink and variable free stream on flow of a viscous incompressible electrically conducting fluid and heat transfer on a non-conducting stretching sheet in the presence of transverse magnetic field near a stagnation point. It has been found that the rate of heat transfer at the sheet increases due to increase in the Prandtl number, while it decreases due to increase in the Hartmann number. Sinha (2014) presented a numerical solution on a MHD stagnation-point flow with heat transfer over a shrinking sheet in the presence of magnetic field. The effects of slip velocity and thermal slip on an electrically conducting viscous incompressible fluid are investigated in this paper. Steady two-dimensional stagnation point flow and heat transfer of a nanofluid over a porous stretching sheet with heat generation is investigated analytically by Malvandi *et al.* (2014). Their results indicate that the reduced Nusselt number declines with increasing in Lewis number whereas the reduced Sherwood number increases. Mahapatra and Gupta (2002) investigated the steady, two-dimensional stagnation-point flow of an incompressible viscous fluid towards a stretching surface. Mahapatra *et al*. (2007) further analyzed the same problem for the MHD flow. The steady two-dimensional stagnation-point flow of a viscous and incompressible fluid over a stretching vertical sheet in its own plane was investigated theoretically by Ishak *et al*. (2006). Unsteady boundary layer flow in the stagnation point region on a stretching flat sheet, where the unsteadiness is caused by the impulsive motion of the free stream velocity and by the suddenly stretched surface, has been analyzed by Nazar *et al*. (2004). Singh *et al*. (2010) considered the convective heat and mass transfer in the presence of the volumetric rate of heat generation/ absorption, which depends on local specie concentration. This work has been extended by Makinde (2012) to include hydro-magnetic mixed convection stagnation point flow with thermal radiation past a vertical plate embedded in a porous medium. Kazem *et al*. (2011) have analytically studied the problem of the two-dimensional stagnation-point flow in a porous medium of a viscous incompressible fluid impinging on a permeable stretching surface with heat generation/absorption.

Motivated by the above studies, we investigate the behavior of MHD mixed convection stagnation-point flow towards a vertical plate embedded in a highly porous medium with heat and mass transfer in the presence of thermal radiation, internal heat generation, Soret and Dufour effects in this paper.

2. MATHEMATICAL ANALYSIS

Consider the MHD steady two-dimensional stagnation-point flow of a viscous incompressible electrically conducting fluid near a stagnation point at a surface coinciding with the plane $y = 0$, the flow being in a region $y > 0$. The configuration and the coordinate system of this stagnation point flow are shown in the Fig. 1. Two equal and opposing forces are applied along the x-axis so that the surface is stretched keeping the origin fixed. The potential flow that arrives from the y-axis and impinges on a flat wall placed at $y = 0$, divides into two streams on the wall and leaves in both the directions. The velocity distribution in the potential flow in the neighborhood of the stagnation point is given by $U_\infty = cx$, where c is a positive constant. A constant magnetic field B_0 is applied in the y direction. Since the magnetic Reynolds number of the flow is taken to be very small, the induced magnetic field is neglected. It is also assumed that the external electric field is zero and the electric field due to polarization of charges is negligible. The temperature and the concentration of the ambient fluid are T_∞ and C_∞ and those at the stretching surface are T_w and C_w respectively.

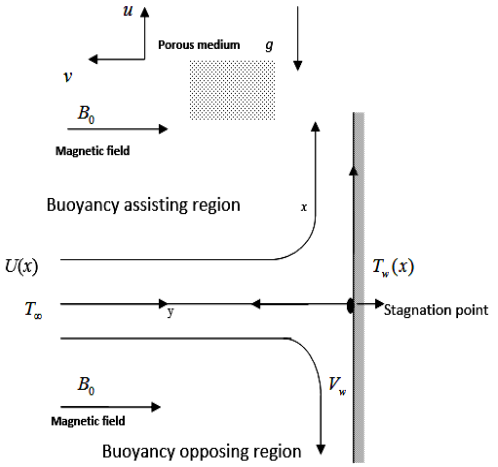

Fig. 1. Physical model and coordinate system.

It is also assumed that the viscous and electrical dissipation are neglected. The MHD equations for two dimensional stagnation-point flow of heat and mass transfer towards a heated vertical plate are

$$\frac{\partial u}{\partial x} + \frac{\partial v}{\partial y} = 0 \qquad (1)$$

$$u\frac{\partial u}{\partial x}+v\frac{\partial u}{\partial y}=\nu\frac{\partial^2 u}{\partial y^2}+g\beta(T-T_\infty)+g\beta^*(C-C_\infty)-\left(\frac{\sigma_e B_0^2}{\rho}+\frac{\nu}{\tilde{K}}\right)(u-U_\infty)+U_\infty\frac{dU_\infty}{dx} \quad (2)$$

$$u\frac{\partial T}{\partial x}+v\frac{\partial T}{\partial y}=\alpha\frac{\partial^2 T}{\partial y^2}-\frac{\alpha}{k}\frac{\partial q_r}{\partial y}+Q(T-T_\infty)+\frac{D_m K_T}{c_s c_p}\frac{\partial^2 C}{\partial y^2} \quad (3)$$

$$u\frac{\partial C}{\partial x}+v\frac{\partial C}{\partial y}=D_m\frac{\partial^2 C}{\partial y^2}+\frac{D_m K_T}{T_m}\frac{\partial^2 T}{\partial y^2}-K_1 C \quad (4)$$

The boundary conditions are

$$u=0,\ v=0,\ T=T_w,\ C=C_w \quad \text{at } y=0$$

$$u\to U_\infty=cx,\ T\to T_\infty,\ C\to C_\infty \text{ as } y\to\infty \quad (5)$$

Using the Rosseland approximation, the radiative heat flux in the y-direction is given by

$$q_r=-\frac{4\sigma^*}{3K'}\frac{\partial T^4}{\partial y} \quad (6)$$

where σ^* and K' are the Stefan-Boltzmann constant and the mean absorption coefficient, respectively. On the assumption that the temperature differences within the flow are sufficiently small, we can express T^4 as a linear function of temperature T_∞ using a truncated Taylor series about the free stream temperature T_∞ as

$$T^4\approx 4T_\infty^3T-3T_\infty^4 \quad (7)$$

We introduce the following non-dimensional variables

$$Gr=\frac{g\beta(T_w-T_\infty)x^3}{\upsilon^2},\quad Gc=\frac{g\beta(C_w-C_\infty)x^3}{\upsilon^2},$$

$$S=\frac{Q\upsilon}{\alpha c},\quad R=\frac{4\sigma^*T_\infty^3}{kK'},\quad Df=\frac{D_m K_T(C_w-C_\infty)}{\alpha c_s c_p(T_w-T_\infty)},$$

$$K=\frac{\upsilon}{c\tilde{K}},\quad \Pr=\frac{\upsilon}{\alpha},\quad Sc=\frac{\upsilon}{D_m},$$

$$M=\frac{\sigma_e B_0^2}{c\rho},\quad \upsilon=\frac{\mu}{\rho}, \quad (8)$$

$$Sr=\frac{K_T(T_w-T_\infty)}{T_m(C_w-C_\infty)},\quad Cr=\frac{K_1}{C},\quad \mathrm{Re}_x=\frac{U_\infty x}{\upsilon},$$

$$Ri_T=\frac{Gr}{\mathrm{Re}_x^2},\quad Ri_C=\frac{Gc}{\mathrm{Re}_x^2}$$

Now we introduce the following similarity transformations as

$$\eta=y\sqrt{\frac{c}{\nu}},\qquad \psi(x,y)=\sqrt{\nu c}\,xf(\eta),$$

$$\theta(\eta)=\frac{T-T_\infty}{T_w-T_\infty},\quad \varphi(\eta)=\frac{C-C_\infty}{C_w-C_\infty} \quad (9)$$

where $\psi(x,y)$ is the stream function defined by $u=\frac{\partial\psi}{\partial y}$ and $v=-\frac{\partial\psi}{\partial x}$ so as to satisfy Eq.(1) identically. By substituting Eqs. (7) - (9) into Eqs. (2) - (5), we obtain the following nonlinear ordinary differential equations:

$$f'''+ff''-f'^2+Ri_T\theta+Ri_C\varphi-(K+M)(f'-1)+1=0 \quad (10)$$

$$\left(1+\frac{4}{3}R\right)\theta''+\Pr f\,\theta'+S\,\theta+Df\,\varphi''=0 \quad (11)$$

$$\varphi''+ScSr\theta''+Scf\,\varphi'-CrSc\varphi=0 \quad (12)$$

where K is the porous medium permeability parameter, R is the thermal radiation parameter, Gr is the local thermal Grashof number, Gc is the local solutal Grashof number, Ri_T is the thermal Richardson number, Ri_C is the solutal Richardson number, Pr is the Prandtl number, Sr is the Soret number, Df is the Dufour number, Sc is the Schmidt number, M is the magnetic field intensity parameter, Cr is the chemical reaction parameter, and S is the internal heat generation parameter. The corresponding boundary conditions (5) now becomes

$$f=0,\quad f'=0,\quad \theta=1,\quad \varphi=1,\quad \text{at}\quad \eta=0,$$
$$f'=1,\quad \theta=0,\quad \varphi=0\quad \text{as}\quad \eta\to\infty. \quad (13)$$

The set of equations (10)-(12) under the boundary conditions (13) have been solved numerically by applying the shooting iteration technique together with Runge-Kutta fourth-order integration scheme. From the process of numerical computation, theskin-friction coefficient, the local Nusselt number and the local Sherwood number are respectively given by

$$C_f=\frac{2\tau_w}{\rho U_\infty^2},\qquad Nu=\frac{xq_w}{k(T_w-T_\infty)},$$

$$Sh=\frac{xq_m}{D_m(C_w-C_\infty)}, \quad (14)$$

where

$$\tau_w=\mu\left.\frac{\partial u}{\partial y}\right|_{y=0}.$$

$$q_w=-k\left.\frac{\partial T}{\partial y}\right|_{y=0}-\left.\frac{4\sigma^*}{3K'}\frac{\partial T^4}{\partial y}\right|_{y=0}, \quad (15)$$

$$q_m=-D\left.\frac{\partial C}{\partial y}\right|_{y=0}.$$

Substituting (7), (8) and (13) into (15), we obtain the expressions for the skin-friction coefficient, the

local Nusselt number and the local Sherwood number as

$$\mathrm{Re}_x^{1/2} C_f = f''(0),$$

$$\mathrm{Re}_x^{-1/2} Nu = -(1+4R/3)\theta'(0), \tag{16}$$

$$\mathrm{Re}_x^{-1/2} Sh = -\varphi'(0).$$

3. RESULTS AND DISCUSSION

Equations (10)-(12) constitute a highly non-linear coupled boundary value problem of third and second order for which the closed-form solution cannot be obtained. Hence the problem has been solved numerically using shooting technique along with fourth order Runge–Kutta scheme. The basic idea of the shooting method for solving boundary value problem is to try to find appropriate initial condition for which the computed solution "hits the target" so that the boundary conditions at the other points are satisfied. Furthermore, the higher order non-linear differential equations are converted into simultaneous linear differential equations of first order and they are further transformed into initial valued problem. The iterative solution procedure was carried out until the error in the solution became less than a predefined tolerance level. We have computed the values of the skin-friction coefficient, the local heat transfer rate and the local mass transfer rate and made a comparison with the corresponding values obtained by Makinde (2012) in Table 1. One can observe that the present results are in good agreement with that of the work by Makinde (2012).

Table 2 presents the variations in the values of the skin-friction coefficient $f''(0)$, the local heat transfer rate $-\theta'(0)$ and the local mass transfer rate $-\varphi'(0)$ for different values of the governing parameters K, M, Ri_T, Ri_C, S, R, Cr, Sr and Df when Pr = 1.0, Sc = 0.5. We observe that the skin-friction at the plate surface increases with increasing values of K, M, Ri_T, Ri_C, S and Df and decreases with increasing values of R, Cr and Sr. It can thus be understood that the influence of magnetic field, buoyancy forces, permeability of porous medium, thermal radiation and Dufour effect tend to increase skin-friction. The rise in the local Nusselt number is seen for increasing values of K and R. But it decreases for increasing values of Ri_T, S, Cr, Sr and Df. Further, we notice that, except for the thermal radiation parameter R, the local Sherwood number increases for increasing values of all other parameters. The effects of the permeability parameter K, magnetic field parameter M, thermal Richardson number Ri_T, solutal Richardson number Ri_C and the heat generation parameter S on the velocity field have been analyzed in Figures 2-6. Figures 7-9 depict the variations of temperature due to the influence of heat generation parameter S, radiation parameter R and Dufour number Df whereas Figures 10 and 11 are plotted for variations of concentration profiles with respect to Sr and Cr.

3.1 Velocity Profiles

The effect of increasing values of K on the velocity profile is presented in Figure 2. It is clear that the velocity decreases gradually on increasing values of K. Fig. 3 shows the influence of magnetic field on the velocity. As M increases, we observe that the velocity also increases and attains its peak value when M = 8 before sliding down rapidly to reach the free stream velocity.

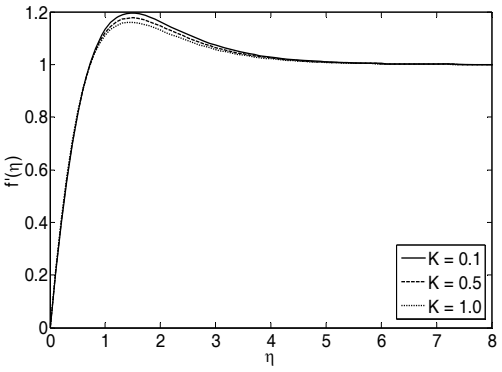

Fig. 2. Velocity profiles for different K values with Cr=0.1, Df=0.2, Ri_T =1, Ri_C =0.5, M=0.1, R=0.1, S=0.1, Sr=0.2.

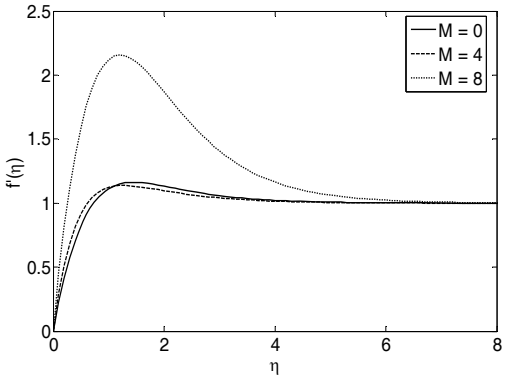

Fig. 3. Velocity profiles for different M values with Cr=0.1, Df=0.2, Ri_T =1, Ri_C =0.5, K=1, R=0.1, S=0.1, Sr=0.2.

For the case of different values of thermal Richardson number Ri_T, the velocity profiles in the boundary layer are shown in Fig. 4. As expected, it is observed that an increase in Ri_T leads to an increase in the values of velocity due to the enhancement in buoyancy force.

Fig. 5 provides the velocity profiles in the boundary layer for various values of the solutal Richardson number Ri_C. This figure indicates that the velocity increases due to the increase in the species buoyancy force. The velocity attains a distinctive maximum in the vicinity of the plate and then decelerates to approach the free stream velocity.

Table 1 Computations showing the comparison with Makinde (2012) for different values of *S* when Ri_T = 1, Ri_c = 0.5, *Pr* = 1, *Sc* = 0.5, *M* = 0, *K* = 0, *Cr* = 0, *Rd* = 0

	$f''(0)$		$-\theta'(0)$		$-\phi'(0)$	
S	Makinde (2012)	Present	Makinde (2012)	Present	Makinde (2012)	Present
-1	1.8444	1.8501	1.3908	1.3897	0.4631	0.4618
0	1.9995	1.9989	0.6932	0.6401	0.4789	0.4761
1	2.1342	2.1299	-0.0730	-0.0727	0.4917	0.4902

Table 2 Values of $f''(0)$, $-\theta'(0)$ and $-\phi'(0)$ for different values of the governing parameters when Pr = 1.0, *Sc* = 0.5

K	*M*	Gr	Gc	*S*	*R*	*Cr*	*Sr*	*Df*	$f''(0)$	$-\theta'(0)$	$-\phi'(0)$
0.1	0.1	1	0.5	0.1	0.1	0.1	0.2	0.2	2.246971	0.097852	0.545198
0.5									2.319502	0.100864	0.545862
1.0									2.415747	0.103737	0.546528
1.0	0	1	0.5	0.1	0.1	0.1	0.2	0.2	2.396287	0.103249	0.546394
	4								3.245195	0.121206	0.550579
	8								4.999324	0.092448	0.565297
1.0	0.1	1	0.5	0.1	0.1	0.1	0.2	0.2	2.415747	0.103737	0.546528
		2							2.968114	0.094643	0.571262
		3							3.507120	0.087987	0.595133
1.0	0.1	1	1	0.1	0.1	0.1	0.2	0.2	2.632905	0.102141	0.555275
			2						3.054221	0.100925	0.571568
			3						3.462389	0.102172	0.586313
1.0	0.1	1	0.5	-0.5	0.1	0.1	0.2	0.2	2.336319	0.554410	0.472620
				0.0					2.399971	0.190934	0.532726
				0.5					2.491805	-0.310545	0.609160
1.0	0.1	1	0.5	0.1	0	0.1	0.2	0.2	2.416824	0.090183	0.548699
					0.5				2.411396	0.135656	0.541185
					1.0				2.410166	0.301118	0.560026
1.0	0.1	1	0.5	0.1	0.1	-1.0	0.2	0.2	2.448736	0.174687	0.034980
						0			2.418123	0.109405	0.507559
						1.0			2.398602	0.058244	0.848120
1.0	0.1	1	0.5	0.1	0.1	0.1	0	0.2	2.415747	0.103737	0.546528
							0.5		2.415123	0.099492	0.570883
							1.0		2.414324	0.092869	0.613600
1.0	0.1	1	0.5	0.1	0.1	0.1	0.2	0	2.407324	0.138510	0.540937
								0.5	2.428890	0.048210	0.555599
								1.0	2.452206	-0.055078	0.572806

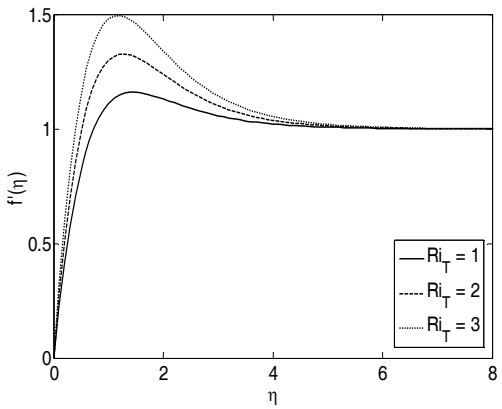

Fig. 4. Velocity profiles for different Gr values with Cr=0.1, Df=0.2, Ri_C =0.5, K=1, M=0.1, R=0.1, S=0.1, Sr=0.2.

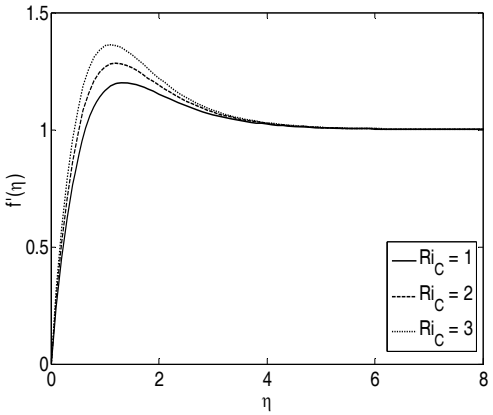

Fig. 5. Velocity profiles for different Gc values with Cr=0.1, Df=0.2, Ri_T =1, K=1, M=0.1, R=0.1, S=0.1, Sr=0.2.

The effect of increasing the internal heat generation parameter *S* on velocity is illustrated in Fig. 6. It is observed that the velocity increases with an increase in the internal heat generation and there is an overshoot in the fluid velocity towards the plate surface. This is due to the fact that the rise in *S* has the tendency to increase the fluid temperature which in turn causes an increased fluid velocity along the plate due to buoyancy effect.

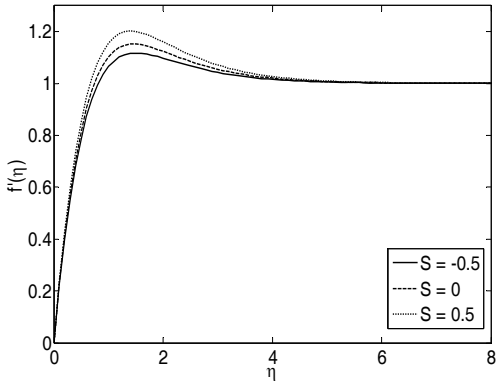

Fig. 6. Velocity profiles for different S values with Cr=0.1, Df=0.2, Ri_T =1, Ri_C =0.5, K=1, M=0.1, R=0.1, Sr=0.2.

3.2 Temperature Profiles

The temperature of the flow suffers a substantial change with the variations of heat generation parameter *S*, radiation parameter *R* and Dufour number *Df*. The effect of heat generation parameter *S* is presented in Fig. 7. Here we notice that there is a steep rise in temperature for the increasing values of *S*. The thermal boundary layer thickness increases with an increase in internal heat generation. An increase in thermal radiation *R* results in an increase in the fluid temperature within the boundary layer is shown in Fig. 8. As a consequence, thermal boundary layer also increases.

The effect of Dufour number *Df* on temperature field is as shown in Fig. 9. From this figure, it is observe that an increase in the Dufour number *Df* increases the temperature inside the boundary layer.

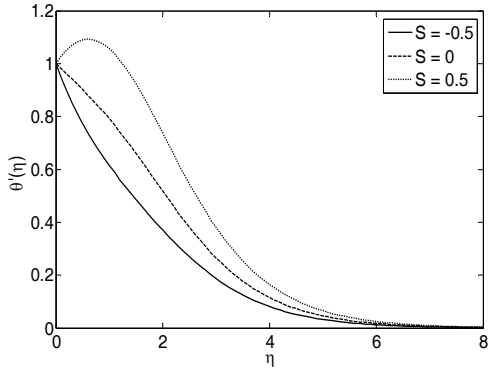

Fig. 7. Temperature profiles for different S values with Cr=0.1, Df=0.2, Ri_T =1, Ri_C =0.5, K=1, M=0.1, R=0.1, Sr=0.2.

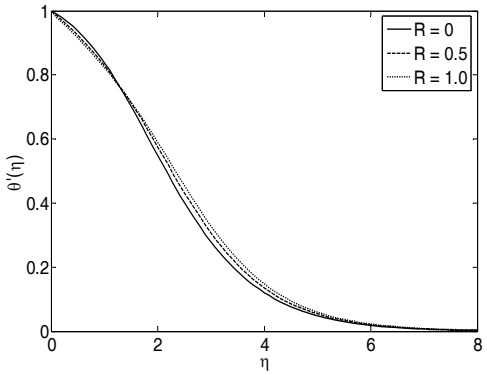

Fig. 8. Temperature profiles for different R values with Cr=0.1, Df=0.2, Ri_T =1, Ri_C =0.5, K=1, M=0.1, S=0.1, Sr=0.2.

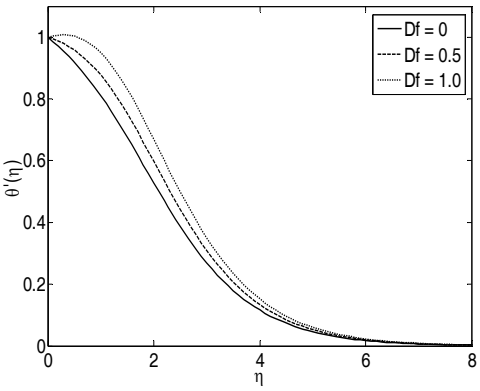

Fig. 9. Temperature profiles for different Df values with Cr=0.1, Ri_T =1, Ri_C =0.5, K=1, M=0.1, R=0.1,S=0.1, Sr=0.2.

3.3 Concentration Profiles

The variations in the concentration boundary layer corresponding to Soret number *Sr* and chemical reaction parameter *Cr* are depicted in Fig. 10 and 11. Figure 10 plots the concentration profiles for different values of *Sr*. As seen from this graph that concentration of species increases with increasing values of the Soret number leading to an increase in thermal boundary value thickness.

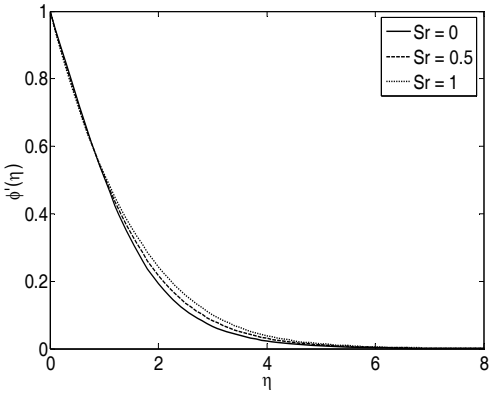

Fig. 10. Concentration profiles for different Sr values with Cr=0.1, Df=0.2, Ri_T =1, Ri_C =0.5, K=1, M=0.1, R=0.1, S=0.1.

It is observed from Fig. 11 that increasing the value of chemical reaction parameter *Cr* decreases the concentration of species in the boundary layer and hence the solutal boundary layer thickness becomes thinner.

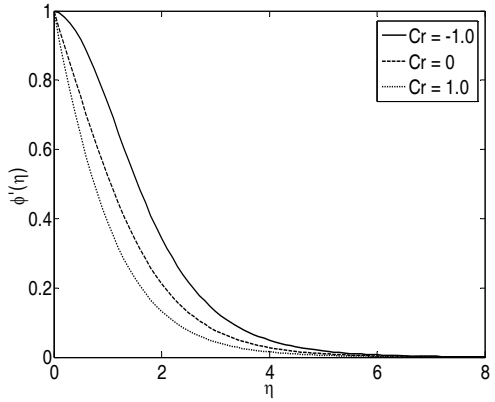

Fig. 11. Concentration profiles for different Cr values with Df=0.2, Ri_T =1, Ri_C =0.5, K=1, M=0.1, R=0.1, S=0.1, Sr=0.2.

4. CONCLUSIONS

In this study, the behavior of MHD mixed convection stagnation-point flow towards a vertical plate embedded in a highly porous medium with heat and mass transfer in the presence of thermal radiation, internal heat generation, Soret and Dufour effects is investigated. The transformed system of non-linear ordinary differential equations is solved numerically by shooting method together with sixth-order Runge-Kutta scheme. From this analysis, the following conclusions are drawn.

(i) The skin-friction coefficient and the local Sherwood number increase with increasing values of magnetic parameter (*M*). For increasing values of internal heat generation (*S*) and Dufour number (*Df*), the skin-friction coefficient and the local Sherwood number increase whereas the local Nusselt number decreases. When the radiation parameter increases, the local Nusselt number and the local Sherwood number increase whereas the skin-friction coefficient decreases.

(ii) The velocity distribution across the boundary layer are increased with an increase in magnetic parameter, thermal Richardson number, solutal Richardson number and then internal heat generation while they show opposite trends with increasing values of the permeability parameter.

(iii) For increasing values of the internal heat generation, thermal radiation and the Dufour number, the temperature increases and hence thermal boundary layer thickness increases.

(iv) The concentration of species increases with increasing Soret number whereas increasing values of chemical reaction parameter decreases the concentration of species in the boundary layer and hence the solutal boundary layer thickness becomes thinner.

ACKNOWLEDGEMENT

One of the authors (S. K) acknowledges the University Grants Commission, India for financial support to carry out this research work under the minor research project No.F MRP-4922/14 (SERO/UGC). One of the authors (S. S) acknowledges the University of Malaya, Malaysia for financial support through the grants RG216-12AFR and RP011B-13AFR.

REFERENCES

Babu, P. R., J. A. Rao and S. Sheri (2014). Radiation effect on MHD heat and mass transfer flow over a shrinking sheet with mass suction. *Journal of Applied Fluid Mechanics* 7(4), 641-650.

Bhuvaneswari, M. and S. Sivasankaran (2014). Free convection flow in an inclined plate with variable thermal conductivity by scaling group transformations. *AIP Conf. Proc.* 1605, 440-445.

Bhuvaneswari, M., S. Sivasankaran and M. Ferdows (2009). Lie group analysis of natural convection heat and mass transfer in an inclined surface with chemical reaction. *Nonlinear Analysis: Hybrid Systems* 3, 536-542.

Bhuvaneswari, M., S. Sivasankaran and Y. J. Kim (2012).Lie group analysis of radiation natural convection flow over an inclined surface in a porous medium with internal heat generation. *Journal of Porous Media* 15(12), 1155-1164.

Chamkha, A. J. and S. E. Ahmed (2011). Similarity solution for unsteady MHD flow near stagnation point of a three-dimensional porous body with heat and mass transfer, heat generation/absorption and chemical reaction. *Journal of Applied Fluid Mechanics* 4(2), 87-94.

Choudhury, R. and S. Kumar Das (2014). Visco-elastic MHD free convective flow through porous media in presence of radiation and chemical reaction with heat and mass transfer. *Journal of Applied Fluid Mechanics* 7(4), 603-609.

Devi, C. D. S., H. S. Takhar and G. Nath (1991). Unsteady mixed convection flow in stagnation region adjacent to a vertical surface. *W¨arme- und Stoff¨ubertragung*, 26(2), 71-79.

Eckert, E. R. G. (1942). Die Berechnung des Wärmeubergangs in der laminaren Grenzschicht umstromter Körper. *VDI Forschungsheft* 416, 1-23.

Gangadhar, K. (2013). Soret and Dufour effects on

hydro magnetic heat and mass transfer over a vertical plate with a convective surface boundary condition and chemical reaction. *Journal of Applied Fluid Mechanics* 6(1), 95-105.

Hayat, T., Z. Abbas, I. Pop and S. Asghar (2010). Effects of radiation and magnetic field on the mixed convection stagnation-point flow over a vertical stretching sheet in a porous medium. *International Journal of Heat and Mass Transfer* 53, 466-474.

Hiemenz, K. (1911). Die Grenzschicht an einem in den gleich formigen flussig keitsstrom eingetacuhten geraden krebzylinder. *Dingl. Polytech. J.* 326, 321-410.

Ishak, A., R. Nazar and I. Pop (2006). Mixed convection boundary layers in the stagnation-point flow toward a stretching vertical sheet. *Meccanica* 4, 509-518.

Karthikeyan, S., M. Bhuvaneswari, S. Rajan and S. Sivasankaran (2013). Thermal radiation effects on MHD convective flow over a plate in a porous medium by perturbation technique. *App. Math. and Comp. Intel*. 2(1), 75-83.

Kazem, S., M. Shaban and S. Abbasbandy (2011). Improved analytical solutions to a stagnation-point flow past a porous stretching sheet with heat generation, *Journal of the Franklin Institute* 348, 2044-2058.

Lee, J., P. Kandaswamy, M. Bhuvaneswari and S. Sivasankaran (2008). Lie group analysis of radiation natural convection heat transfer past an inclined porous surface. *Journal of Mechanical Science and Technology* 22, 1779-1784.

Mahapatra, T. R. and A. S. Gupta (2002). Heat transfer in a stagnation-point flow towards a stretching sheet. *Heat and Mass Transfer* 38, 517-521.

Mahapatra, T. R., S. Dholey and A. S. Gupta (2007). Momentum and heat transfer in the magneto-hydrodynamic stagnation-point flow of a viscoelastic fluid toward a stretching surface. *Meccanica* 42, 263-272.

Makinde, O. D. (2012). Heat and mass transfer by MHD mixed convection stagnation point flow toward a vertical plate embedded in a highly porous medium with radiation and internal heat generation. *Meccanica* 47, 1173-1184.

Malvandi, A, F. Hedayati and M. R. H. Nobari (2014). An HAM analysis of stagnation-point flow of a nanofluid over a porous stretching sheet with heat generation. *Journal of Applied Fluid Mechanics* 7(1), 135-145.

Mukhopadhyay, S. (2009). Effects of radiation and variable fluid viscosity on flow and heat transfer along a symmetric wedge. *Journal of Applied Fluid Mechanics* 2(2), 29-34.

Nazar, R., N. Amin and I. Pop (2004). Unsteady mixed convection boundary layer flow near the stagnation point on a vertical surface in a porous medium. *Int. J. Heat Mass Transfer* 47, 2681–2688.

Nazar, R., N. Amin, D. Filip and I. Pop (2004). Unsteady boundary layer flow in the region of the stagnation point on a stretching sheet. *International Journal of Engineering Science*, 42, 1241-1253.

Postelnicu, A. (2010). Heat and mass transfer by natural convection at a stagnation point in a porous medium considering Soret and Dufour effects. *Heat Mass Transfer* 46,831-840.

Seth, G. S., S. Sarkar, S. M. Hussain and G. K. Mahato (2015). Effects of Hall current and rotation on hydromagnetic natural convection flow with heat and mass transfer of a heat absorbing fluid past an impulsively moving vertical plate with ramped temperature. *Journal of Applied Fluid Mechanics* 8(1), 159-171.

Sharma, P. R. and G. Singh (2009). Effects of variable thermal conductivity and heat source /sink on MHD flow near a stagnation point on a linearly stretching sheet. *Journal of Applied Fluid Mechanics* 2(1), 13-21.

Singh, G., P. R. Sharma and A. J. Chamkha (2010). Effect of volumetric heat generation /absorption on mixed convection stagnation point flow on an isothermal vertical plate in porous media. *Int. J. Industrial Mathematics* 2(2), 59-71.

Sinha, A. (2014). Steady stagnation point flow and heat transfer over a shrinking sheet with induced magnetic field. *Journal of Applied Fluid Mechanics* 7(4), 703-710.